

Synthesis and Double Doping Behavior of a Poly(*p*-phenylenevinylene)s Bearing Conjugated Side Chains

Hirotsugu Kawashima, Kohsuke Kawabata, Hiromasa Goto

Graduate School of Pure and Applied Sciences, Institute of Materials Science, University of Tsukuba, Tsukuba, Ibaraki 305-8573, Japan
Correspondence to: H. Goto (E-mail: gotoh@ims.tsukuba.ac.jp)

Received 22 September 2011; accepted 2 January 2012; published online 31 January 2012

DOI: 10.1002/pola.25919

ABSTRACT: A poly(*p*-phenylenevinylene) derivative bearing conjugated side chains (polyCPV) was synthesized by Migita-Kosugi-Stille type coupling polycondensation reaction. This polymer contains phenylenevinylene units in both the main chain and the side chains. UV-vis absorption and fluorescence emission spectroscopies revealed a well-developed π -conjugation of the polyCPV. The absorption band of the polymer was extended to long wavelengths. A fluorescent emission maximum of polyCPV is located at considerably

longer wavelengths than that of the conjugated side chain monomer. Electron spin resonance measurements of poly CPV confirmed generation of charge species in both the main chain and the side chains via iodine doping. © 2012 Wiley Periodicals, Inc. *J Polym Sci Part A: Polym Chem* 50: 1530–1538, 2012

KEYWORDS: atomic force microscopy (AFM); conjugated polymers; ESR/EPR; UV-vis spectroscopy

INTRODUCTION Conjugated polymers have attracted much attention because of their characteristic optical and electrochemical properties.^{1–6} Many kinds of conjugated polymers have been synthesized for various applications, such as organic photovoltaic cells, organic light-emitting diodes, and field-effect transistors.^{7–11}

Photo-induced electron transfer in composite of conducting polymers has been studied for conjugated polymers such as poly (*para*-phenylenevinylene) (PPV) and C₆₀, and its derivatives. The charge transfer process is fast and has good efficiency.^{12,13} This system is driven by intermolecular interaction between PPV as an electron donor and C₆₀ as an electron acceptor.

Introduction of flexible side chains to conjugated polymers improves solubility of resulting polymers. Furthermore, introduction of liquid crystalline substituent onto rigid conjugated main chain increases solubility and processability and self-alignable properties.^{14,15} However, in this case, charge transfer between side chain and main chain cannot be expected. On the other hand, we assumed that introduction of conjugated side chains to conjugated polymers affords intramolecular interaction between side chain and main chain. This system affords light accumulation through energy capturing from the conjugated side chain. Long conjugated side chains increase susceptibility of photon energy from outside environment.

As for main chain–side chain-type conjugated polymers, polarons as a charge carrier can be generated by electron

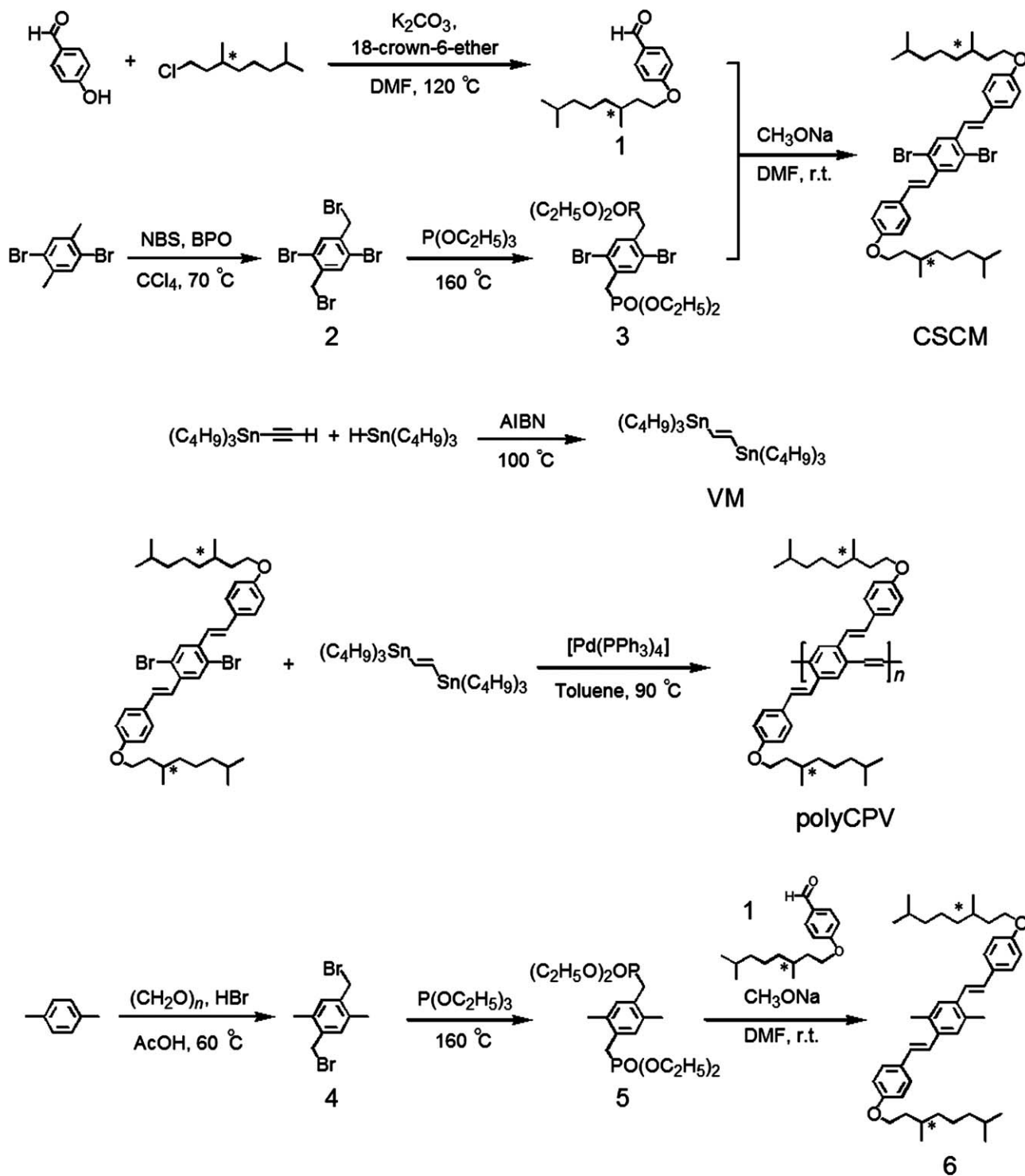
accepter doping in both the side chain and the main chain, and stabilization of the polarons along the main chain may be expected via corporation of the side chain. Two dimensionally distributed polarons in both side chain direction and main chain direction may be obtained for the polymers.

Conjugated polymers bearing conjugated side chains have large π -conjugated system distributed from main chain to the side chain.^{16,17} To date, several studies of conjugated side chain polymers have been reported,^{16–19} and applications for organic electronic devices based on conjugated polymers have been carried out.^{20,21} These polymers have advantages for extension of absorption bands to long wavelengths, and tunability of band gaps with introduction of conjugated substituents. Intramolecular electronic communication between the main chain and the side chain through conjugation structures of the polymers are possible. On the other hand, drawbacks such as low solubility, difficulty of construction of the main-chain/side-chain conjugated architecture due to rigid bulky side chains still remain. Therefore, a new synthetic strategy and characterization for main-chain/side-chain conjugated polymers are further required.²²

In this research, we synthesized a conjugated main-chain/side-chain polymer which has phenylenevinylene units in both the main chain and the side chain. Generally, conjugated polymers show low solubility because of rigid and highly developed π -conjugation. The PPV backbone is known as

Additional Supporting Information may be found in the online version of this article.

© 2012 Wiley Periodicals, Inc.



SCHEME 1 Synthetic routes to poly(*p*-phenylenevinylene) bearing conjugated side chains (polyCPV) and CSCM derivative (6). DMF, *N,N*-dimethylformamide; NBS, *N*-bromosuccinimide; BPO, benzoyl peroxide; AIBN, *N,N*-azobisisobutyronitrile.

comparatively flexible structure among the conjugated polymers.²³ We synthesized a PPV having conjugated side chains to improve solubility, and expect electronic communication between the main chain and the side chains. Optical properties and vapor-phase iodine doping of the main-chain/side-chain-type conjugated polymer were further examined.

RESULTS AND DISCUSSION

Synthesis and Processability

Synthetic routes to poly(*p*-phenylenevinylene) bearing conjugated side chains (polyCPV) are shown in Scheme 1. Williamson etherification with an aid of crown ether as a phase-transfer catalyst afforded compound **1**. Next, the

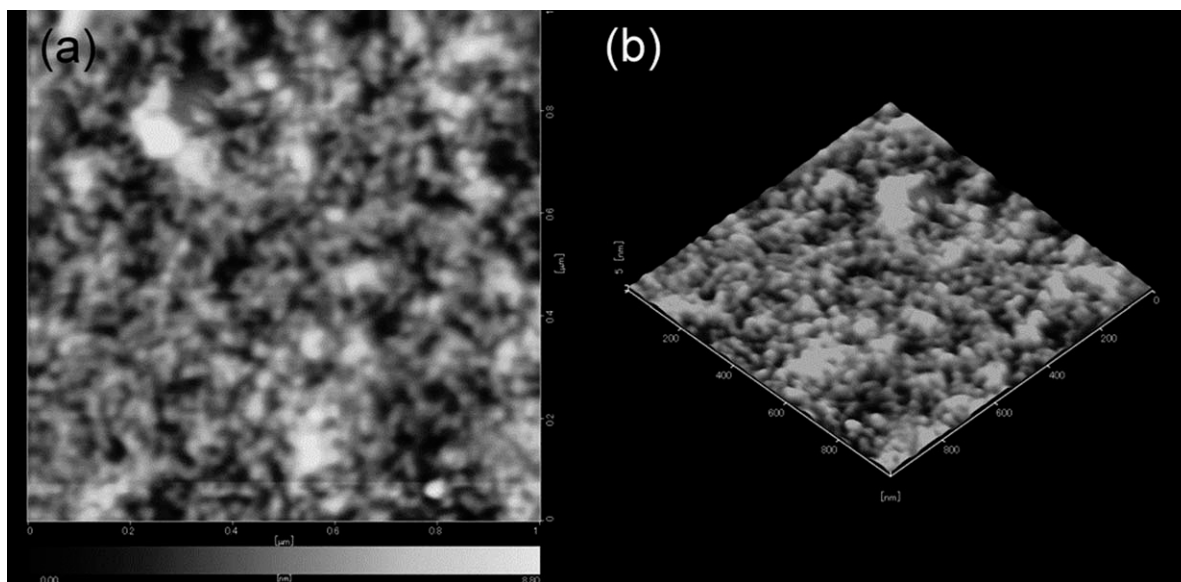


FIGURE 1 AFM two-dimensional (a) and three-dimensional (b) images of polyCPV film spin-cast from CHCl_3 . This is a phase image acquired in tapping mode.

aldehyde group in compound 1 was reacted with the phosphonate ester groups of compound 3, according to Horner-Wadsworth-Emmons reaction. 1,2-Bis(tributyltin ethylene (vinylene monomer, VM) was synthesized using azobisisobutyronitrile. Finally, the conjugated side chain monomer (CSCM) and VM were copolymerized by the Migita-Kosugi-Stille coupling reaction. CSCM derivative (6) was also prepared as a reference material for ESR measurement. A detailed synthetic procedure is described in the Experimental section, and proton NMR spectra of these compounds are shown in Supporting Information Figures S1–S6.

Integrals of the proton NMR spectrum of polyCPV show good agreement with theoretical values (Supporting Information Fig. S6). This result indicates that the polycondensation reaction afforded the desired polymer. PolyCPV is red, while CSCM is yellow (Supporting Information Fig. S7). Gel permeation chromatography (GPC) measurements indicated the number average molecular weight (M_n) of 8600, the weight average molecular weight (M_w) of 19,700, and the polydispersity (M_w/M_n) of 2.29.

Generally, conjugated polymers having conjugated side chains show low solubility as compared to polymers with alkyl side chains because of their bulky structure.^{24,25} PolyCPV, however, dissolves in chloroform, tetrahydrofuran (THF), and toluene probably due to a flexibility of conjugated structure of phenylenevinylene. Furthermore, chirality of alkyl groups in the side chains can provide a further good film-forming property.²⁶

Atomic force microscopy (AFM) observation for polyCPV film reveals surface of the film showing pebbles like structure, as shown in Figure 1. Differential scanning calorimeter measurements were examined for polyCPV (Supporting Information Fig. S8). No phase transition was observed in the range

of 30–300 °C. The bulky side chains may depress formation of liquid crystal.

Optical and Electrochemical Properties

Figure 2 shows UV-vis absorption and fluorescence spectra of polyCPV. Absorption maxima of polyCPV and CSCM are at 339 nm (Table 1). PolyCPV also shows an absorption shoulder at 448 nm. This indicates that the absorption maximum at 339 nm is due to π - π^* transition of *p*-distyrylbenzene moiety in the CSCM unit, and the shoulder at 448 nm of polyCPV is due to π - π^* transition of the main chain. Although absorption maxima of polyCPV and CSCM are located at the same wavelength, polyCPV shows an emission maximum at longer wavelengths than that of CSCM. Therefore, polyCPV displays the emission from the conjugated main chain rather than from the conjugated side chain. These results indicate that polyCPV harvests photon energy from the conjugated side chains and emits fluorescence from the conjugated main chain. That is, energy conduction from the conjugated side chain to the main chain can be occurred

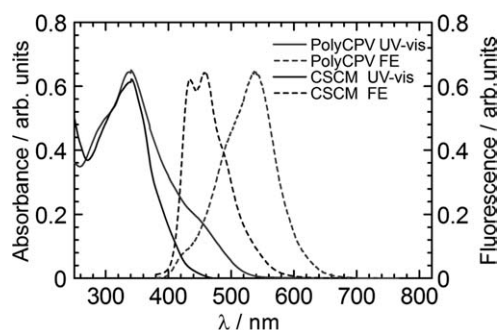


FIGURE 2 UV-vis absorption (solid) and fluorescence emission (dashed) spectra of PolyCPV (gray) and CSCM (black).

TABLE 1 Maximum Absorption, Emission^a, and Absolute Quantum Yields of PolyCPV and CSCM

	λ_{max} (nm)	Em_{max} (nm)	$\Phi_{\text{fe}}^{\text{b}}$	$\Phi_{\text{fi}}^{\text{c}}$
PolyCPV	339/448 (sh)	537	0.23	0.10
CSCM	339	434, 458	0.11	0.02

^aExcitation wavelength is 360 nm.

^b Φ_{fe} = external quantum efficiency.

^c Φ_{fi} = internal quantum efficiency.

in polyCPV. Excitation spectrum of polyCPV illustrated a similar shape with the absorption spectrum of polyCPV (Supporting Information Fig. S9). Absolute fluorescent quantum yields of CSCM and polyCPV solution in chloroform were estimated (Table 1). The results showed improvement of the internal and external quantum efficiencies due to so-called polymer effect. Visual images of fluorescence emissions of the polyCPV and CSCM derivative (Compound 6) are shown in Figure 3 (Supporting Information Fig. S10).

Cyclic voltammetry measurements for monomer CSCM and PolyCPV (cast film on Pt) were carried out in acetonitrile solution containing 0.1 M tetrabutylammonium perchlorate at a scan rate of 100 mV/s. An oxidation peak of polyCPV with an onset of $E_{\text{ox/onset}} = 0.52$ V (vs. Fc/Fc⁺) was observed. The HOMO level (E_{HOMO}) of polyCPV was estimated to be -5.27 eV. The lowest unoccupied molecular orbital (LUMO) of polyCPV is estimated to be -2.89 eV, calculated from the highest occupied molecular orbital (HOMO) energy level and optical bandgap $E_{\text{g}} (= 2.38$ eV). Electrochemical onset potentials, optical absorption onset wavelengths, and electronic energy levels of CSCM and polyCPV are summarized in Table 2. These values are well matched with the previously reported results of alkoxy-substituted poly(*p*-phenylenevinylene) derivatives.^{27–29}

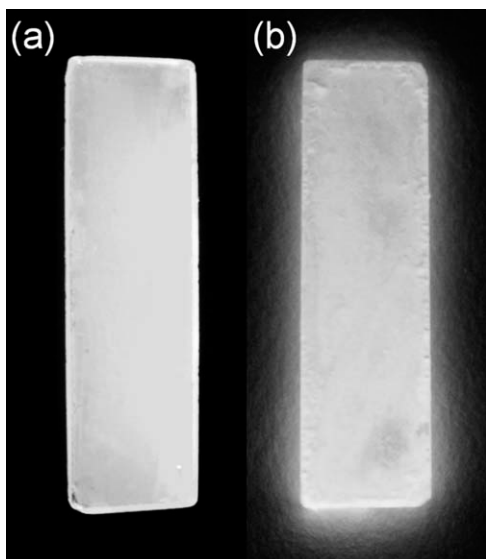


FIGURE 3 Fluorescent emissions of PolyCPV (cast film on quartz substrate) (a) and compound 6 (cast film on quartz substrate) (b).

TABLE 2 Electrochemical Onset Potentials, Optical Absorption Onset Wavelengths, and Electronic Energy Levels of PolyCPV and CSCM

	$E_{\text{ox/onset}}$ (V)	E_{HOMO} (eV)	λ_{onset} (nm)	$E_{\text{g}}^{\text{opt}}$ (eV)	E_{LUMO} (eV)
PolyCPV	0.52	-5.27	521	2.38	-2.89
CSCM	0.47	-5.22	443	2.80	-2.42

Electron Spin Resonance Measurements

Next, we discuss generation of charge species of polyCPV in both main chain and the side chains. *In situ* doping property of polyCPV was examined by electron spin resonance (ESR) spectroscopy. Conjugated polymers before doping are insulators because π -electrons of the polymers have almost no mobility along the backbone. In this condition, no charge carriers, such as holes and excess electrons, exist in the polymer. A doping process allows a generation of charge carriers for a π -conjugated system of the conjugated polymers. This doping process produces a pair of a free radical and a positive charge along the polymer chain, and this pair behaves as a charge carrier (Supporting Information Fig. S10). This pair is referred to as polarons for conducting polymers. The ESR spectroscopy can detect free radicals of the polarons and allows us to discuss the charged states of conjugated polymers.³⁰

Figure 4(a–d) shows ESR spectra for polyCPV with *in situ* vapor-phase doping of iodine. Line shape of the ESR signal changed drastically with time. During the initial stage of doping, a sharp and almost symmetric signal grew with doping time [Fig. 4(b)]. This stage is designated to be Phase I in this study. *g*-Value of a signal at the initial stage Phase I was 2.0032. This value is somewhat low for a conjugated polymer. During the next stage, determined to as Phase II, the symmetrical signal shape gradually changed [Fig. 4(c)]. Intensity of the upward peak decreased and the peak shifted to low magnetic fields with the doping time, although the trough remained in the same position. During the Phase II, *g*-value of the doped polyCPV also increased to 2.0043 in 60 min. In the next stage, the peak height increased again after the doping time of 60 min [Fig. 4(d), Phase III] suggesting generation of a new signal in the entire ESR signal due to generation of another charge carrier. After 300 min of the iodine doping, the ESR signal appeared to be saturated. *g*-Value of the signal was 2.0049 after 300 min of the doping time. This value matched well the reported values for polaron states of normal poly(*p*-phenylenevinylene) derivatives.^{31,32} Figure 5 shows *g*-value, ESR intensity, and peak width plots versus doping time which describe the distinct behavior of paramagnetic properties of polyCPV. This is a unique example of the doping behavior observed in the ESR.

To verify this unique behavior on doping of polyCPV, we conducted ESR measurements for compound 6 as a reference under the same conditions, as shown in Figure 6. This compound exhibited a sharp signal after vapor-phase doping of iodine. Peak position of the ESR signals shows no change during the iodine doping, and *g*-value of compound 6 was constant

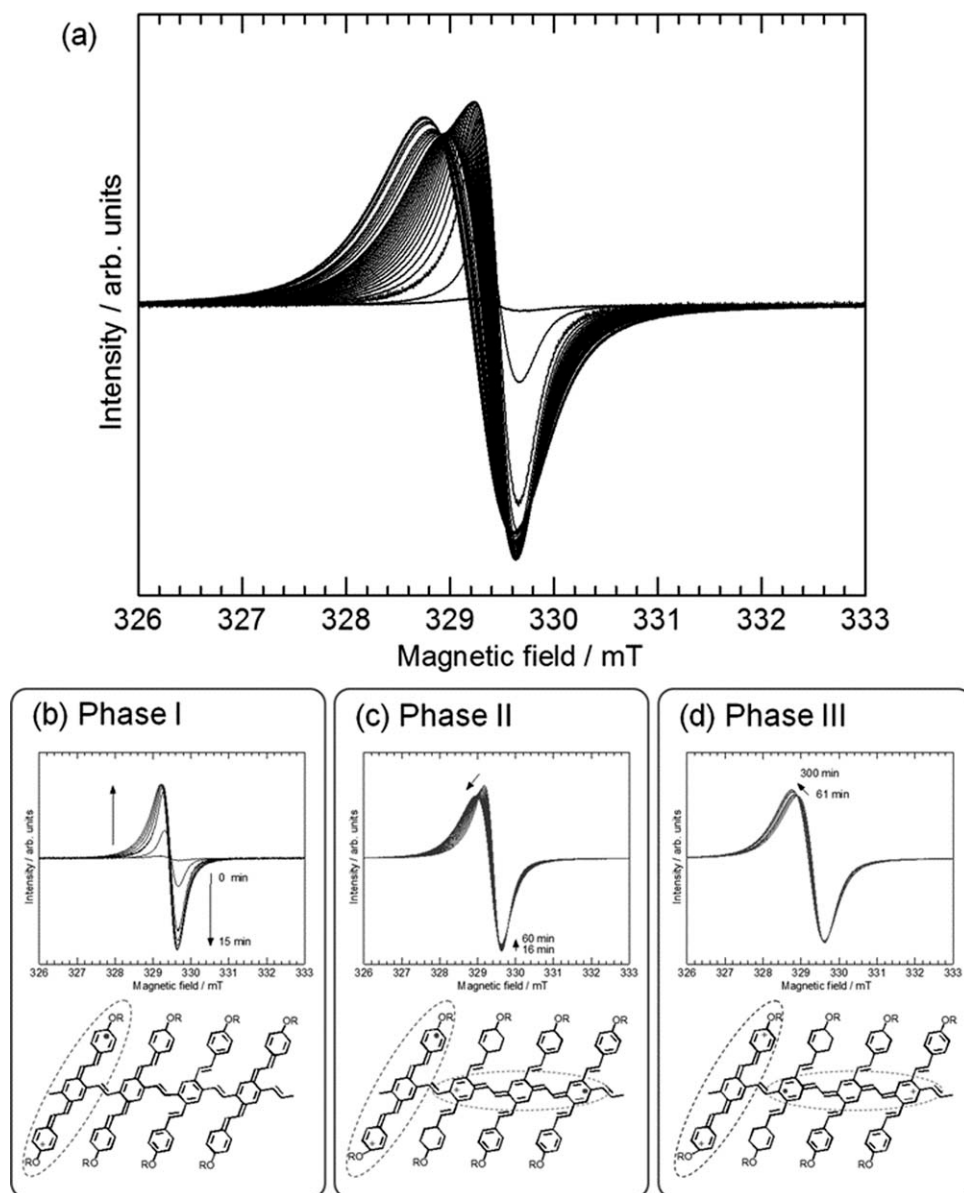


FIGURE 4 ESR spectra of polyCPV after vapor-phase iodine doping for (a) 0–300 min, (b) 0–15 min, (c) 16–60 min, and (d) 61–300 min.

($g = 2.0035$). This value was close to that of polyCPV at the Phase I. From these results, two different types of unpaired electrons can be generated in the entire polymer system of polyCPV. The signals observed in the Phase I for polyCPV may be explained by generations of radicals in the conjugated side chains, while the ESR signal in the heavily doped state may be associated with the charge carriers in the main chain of the polyCPV. The conjugated side chains of polyCPV are initially doped during early stages of the iodine doping, and then, the main chain doping occurs in a subsequent stage. This side chain doping and main chain doping behavior can be referred to as “double doping process.” Overlaps between the two ESR signals produce the apparent asymmetric shapes of the observed spectra during the transition between these two phases.

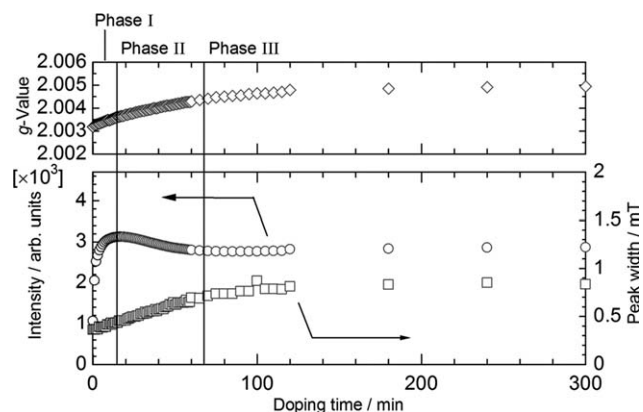


FIGURE 5 g -Value, ESR intensity, and peak width plots of polyCPV as a function of vapor-phase iodine doping time.

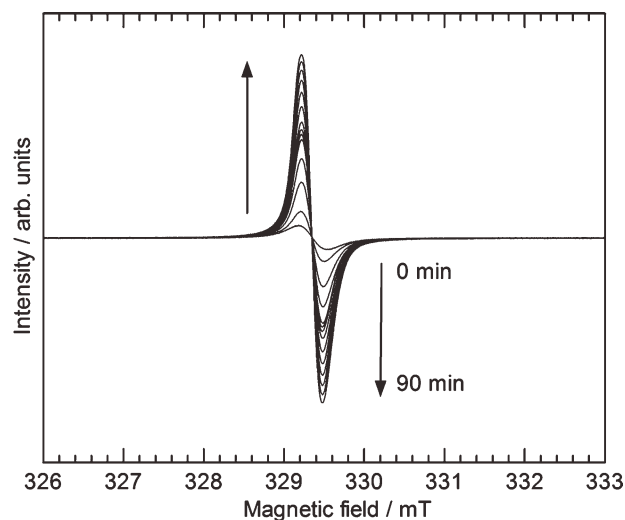


FIGURE 6 ESR spectra of the CSCM derivative (6) after vapor-phase iodine doping for 0–90 min.

Generally, a highly developed π -conjugated polymers display low ionization potential.³³ As a result, long effective conjugation allows good dopable property. In the case of

polyCPV, the main chain is characterized by a long conjugation length as compared to the conjugated side chain. Therefore, the main chain may be first doped preferentially before the doping of the side chain. However, the experimental results of ESR measurements suggested a different conclusion. Therefore, the entire shape of the individual polymer chain needs to be considered for explanation of this result.

Bulky side chains in polyCPV wrap around the main chain as shown in Figure 7. In this arrangement, iodine could not easily penetrate space between the side chains. Iodine is not accessible to the main chains in the early stage of doping because of a mechanical shielding by the side chains. On the other hand, the conjugated side chains are located on outside of the main chain, which can have good contact with vapor-phase iodine. Consequently, the side chains are doped first and the main chains are gradually doped next. The two charge carriers may exist independently in the side-chain/main-chain-conjugated system. Therefore, two dimensionally spread polarons in both main chain and side chains directions can be generated by the heavy doping.

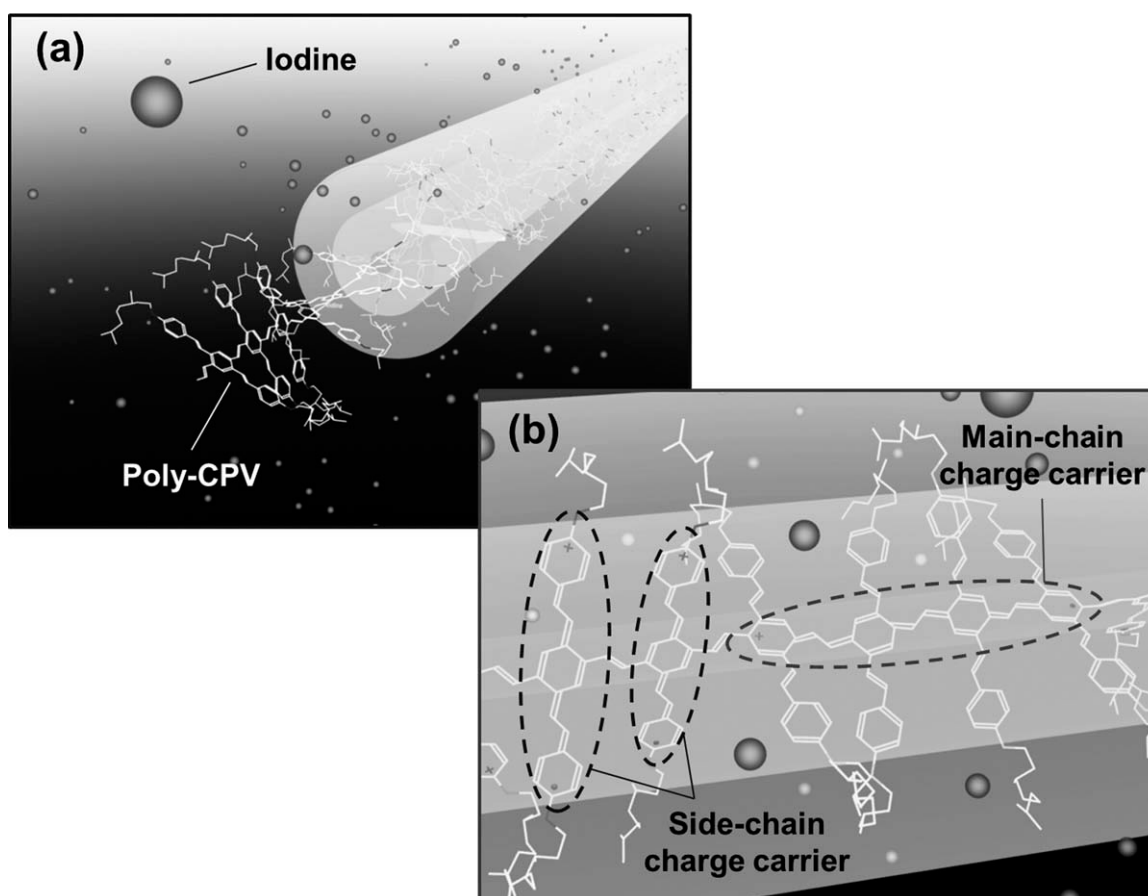


FIGURE 7 Double doping model of iodine. (a) Restriction of iodine access to the conjugated main chain of polyCPV due to bulky side chain pseudolayers during the early doping stage (Phase I). (b) Main chain and side chain polarons generated by double-doping during the heavy doping stage (Phases II and III).

EXPERIMENTAL**Materials and Instruments**

All reagents were purchased from Kanto, Tokyo Kasei, and Wako and used as received. ^1H NMR spectra of low molecular compounds were taken on ECS 400 spectrometer (JEOL) with chloroform- d^1 at room temperature. ^1H NMR spectrum of polyCPV was taken by AVANCE-600 NMR spectrometer (Bruker) with chloroform- d^1 at 60 °C. Chemical shifts are reported in ppm downfield from tetramethylsilane (TMS), using the solvent's residual signal as an internal reference. Matrix-assisted laser desorption ionization time of flight (MALDI-TOF) mass spectra were recorded on a TOF/TOF 5800 (AB Sciex). Molecular weights of the polymers were determined by GPC with 5 μm -MIXED-D column (Polymer Laboratories), PU-980 HPLC pump (Jasco), and MD-915 multiwavelength detector (Jasco), with THF used as the solvent, with the instruments calibrated by polystyrene standard. UV-vis absorption spectra were recorded on a V-630 UV-vis optical absorption spectrometer (Jasco). Photoluminescence spectra were recorded on F-4500 fluorescence spectrophotometer (Hitachi). Absolute fluorescent quantum yields of compounds were measured with FP8500 (Jasco). ESR spectra were taken at room temperature using JES-TE200 ESR spectrometer (JEOL) during *in situ* vapor-phase doping process with iodine.

Synthesis**Synthesis of 4-(3,7-Dimethyloctyloxy)benzaldehyde (1)**

A solution of 4-hydroxybenzaldehyde (0.704 g, 5.76 mmol), 18-crown-6-ether (0.099 g, 0.38 mmol), potassium carbonate (0.797 g, 5.77 mmol), *N,N*-dimethylformamide (DMF) (3 mL) was stirred. Then, 1-chloro-3,7-dimethyloctane (1.15 g, 6.49 mmol) was added to the reaction mixture and refluxed for 16 h at 120 °C. The reaction was monitored by thin layer chromatography (TLC). The mixture was dissolved in dichloromethane, washed with water thoroughly, extracted by dichloromethane, and dried over MgSO_4 . After filtration, the solvent was removed *in vacuo* and the crude material was purified by column chromatography (silica gel, ethyl acetate). The product was dried *in vacuo* and isolated as a colorless liquid (1.20 g, 4.57 mmol, 79% yield).

^1H NMR (400 MHz, δ from TMS (ppm), CDCl_3): δ 0.87 (d, 6H, $-\text{CH}(\text{CH}_3)_2$, $J = 6.6$ Hz), 0.95 (d, 3H, $-\text{CH}(\text{CH}_3)-\text{CH}_2-$, $J = 6.4$ Hz), 1.18 (m, 6H, $-\text{CH}(\text{CH}_3)-(\text{CH}_2)_3-$), 1.53 (m, 1H, $-\text{CH}(\text{CH}_3)-$), 1.65 (m, 2H, $\text{O}-\text{CH}_2-\text{CH}_2-$), 1.84 (m, 1H, $-\text{CH}(\text{CH}_3)_2$), 4.07 (t, 2H, $-\text{O}-\text{CH}_2-$, $J = 6.8$ Hz), 6.99 (d, 2H, 3,5H, $J = 8.7$ Hz), 7.82 (d, 2H, 2,6H, $J = 8.7$ Hz), 9.87 (s, 1H, $-\text{CHO}$).

Synthesis of 1,4-Dibromo-2,5-bis-bromomethylbenzene (2)

A solution of 1,4-dibromo-2,5-dimethylbenzene (2.01 g, 7.60 mmol), *N*-bromosuccinimide (2.70 g, 15.2 mmol), and tetrachloromethane (18 mL) was stirred. Then, benzoyl peroxide (0.017 g, 0.071 mmol) was added, and the reaction mixture was refluxed for 24 h at 70 °C. The reaction was monitored by TLC. The crude product was washed with water several times, extracted by dichloromethane, and dried over MgSO_4 . After filtration, the solvent was removed *in vacuo*, and the

desired material was purified by recrystallization from *n*-hexane to afford a white solid (0.751 g, 1.78 mmol, 31% yield).

^1H NMR (400 MHz, δ from TMS (ppm), CDCl_3): δ 4.54 (s, 4H, $-\text{CH}_2\text{Br}$), 7.66 (s, 2H, 3,6H).

Synthesis of 1,4-Dibromo-2,5-bis-(diethylphosphinoylmethyl)benzene (3)

A solution of 1,4-dibromo-2,5-bis-bromomethylbenzene (0.749 g, 1.78 mmol) and triethyl phosphite (0.61 mL, 3.56 mmol) was refluxed for 12 h at 160 °C, then unreacted triethyl phosphite was removed by evaporation under reduced pressure. The desired material was purified by recrystallization from ethyl acetate to afford a pale yellow solid (0.854 g, 1.59 mmol, 90% yield).

^1H NMR (400 MHz, δ from TMS (ppm), CDCl_3): δ 1.28 (t, 12H, $-\text{OCH}_2\text{CH}_3$, $J = 7.1$ Hz), 3.33 (d, 4H, $\text{Ar}-\text{CH}_2-\text{P}-$, $J_{\text{P-H}} = 20.6$ Hz), 4.07 (sept, 8H, $-\text{O}-\text{CH}_2-\text{CH}_3$, $J = 7.1$ Hz), 7.64 (d, 2H, 3,6H, $J = 1.8$ Hz).

Synthesis of CSCM

Sodium methoxide (0.812 g, 15.0 mmol) was added in a solution of 1,4-dibromo-2,5-bis-(diethylphosphinoylmethyl)benzene (0.796 g, 1.48 mmol) in DMF (5 mL) under N_2 atmosphere at 0 °C and stirred for 30 min. After the color of the mixture changed from red to green, 4-(3,7-dimethyloctyloxy)benzaldehyde (0.790 g, 3.01 mmol) was added dropwise to the mixture and stirred for 2 h at rt. The reaction was monitored by TLC. Then, the mixture was washed with water, extracted by dichloromethane, and dried over MgSO_4 . After filtration, the solvent was removed *in vacuo*, and the crude product was purified by column chromatography (silica gel, chloroform). The compound was dried *in vacuo* to afford a yellow solid (0.778 g, 1.03 mmol, 70% yield).

^1H NMR (400 MHz, δ from TMS (ppm), CDCl_3): δ 0.88 (d, 12H, $-\text{CH}(\text{CH}_3)_2$, $J = 6.6$ Hz), 0.95 (d, 6H, $-\text{CH}(\text{CH}_3)-\text{CH}_2-$, $J = 6.4$ Hz), 1.13–1.88 (m, 20H, $\text{O}-\text{CH}_2-\text{CH}_2-\text{CH}(\text{CH}_3)-(\text{CH}_2)_3-\text{CH}(\text{CH}_3)_2$), 4.02 (t, 4H, $-\text{O}-\text{CH}_2-\text{C}_9\text{H}_{19}$, $J = 6.8$ Hz), 6.90 (d, 4H, 3,5H (side chain benzene) $J = 8.7$ Hz), 6.99 (d, 2H, $\text{Ar}-\text{CH}=\text{CH}-\text{Ar}-\text{O}-$, $J = 16.0$ Hz), 7.21 (d, 2H, $\text{Ar}-\text{CH}=\text{CH}-\text{Ar}-\text{O}-$, $J = 16.0$ Hz), 7.47 (d, 4H, 2,6H (side chain benzene), $J = 8.7$ Hz), 7.83 (s, 2H, 3,6H).

^{13}C NMR (100 MHz, δ from TMS (ppm), CDCl_3): δ 19.7, 22.6, 24.6, 28.0, 29.8, 36.2, 37.3, 39.2, 66.4, 114.8, 123.4, 128.2, 129.1, 129.2, 129.9, 131.6, 137.2, 159.4. MALDI-TOF MASS: calcd for $\text{C}_{42}\text{H}_{56}\text{Br}_2\text{O}_2$, 752.70; found, 752.27.

Synthesis of 1,2-Bis-(tributylstannyl)ethylene (Vinylene Monomer)

A solution of tributylstannyl acetylene (3.90 g, 11.9 mmol), tributylstannyl hydride (3.46 g, 11.9 mmol), and azobisisobutyronitrile (0.039 g, 0.24 mmol) was refluxed for 6 h at 100 °C. The reaction was monitored by TLC. Then, the crude product was washed with water, extracted by dichloromethane, and dried over MgSO_4 . After filtration, the solvent was removed *in vacuo*. Unreacted materials were removed by evaporation under reduced pressure to obtain pure product.

The product was afforded a colorless liquid (6.58 g, 10.9 mmol, 91.7% yield).

^1H NMR (400 MHz, δ from TMS (ppm), CDCl_3): δ 0.80–0.96 (m, 30H, $\text{Sn-CH}_2\text{CH}_2\text{CH}_2\text{CH}_3$), 1.31 (sext, 12H, $\text{Sn-CH}_2\text{CH}_2\text{CH}_2\text{CH}_3$, $J = 7.3$ Hz), 1.50 (quint, 12H, $\text{Sn-CH}_2\text{CH}_2\text{CH}_2\text{CH}_3$, $J = 7.9$ Hz), 6.87 (s, 2H, H-C=C-H).

PolyCPV

A solution of CSCM (0.149 g, 0.198 mmol) and VM (0.124 g, 0.204 mmol) in toluene (3 mL) are stirred for 30 min at 50 °C. Then, tetrakis(triphenylphosphine)palladium (0.009 g, 0.008 mmol) was added to the solution and refluxed for 2 days at 90 °C. After cooling, the mixture was poured into methanol (50 mL) and washed. The washing procedure was repeated in three times. The precipitates were isolated by suction filtration, and dried *in vacuo* to afford a red solid (0.071 g, 0.115 mmol, 58% yield).

^1H NMR (600 MHz, δ from TMS (ppm), CDCl_3): δ 0.87 (brs, 12H, $-\text{CH}(\text{CH}_3)_2$), 0.95 (m, 6H, $-\text{CH}(\text{CH}_3)-\text{CH}_2-$), 1.09–1.81 (br, m, 20H, $\text{O-CH}_2-\text{CH}_2-\text{CH}(\text{CH}_3)-(\text{CH}_2)_3-\text{CH}(\text{CH}_3)_2$), 3.97 (brs, 4H, $-\text{O-CH}_2-\text{C}_9\text{H}_{19}$), 6.00–7.90 (brm, 16H, Ar-CH=CH-Ar (main chain), Ar-CH=CH-Ar (side chain), 3,6H (main chain benzene), 3,5H (side chain benzene), 2,6H (side chain benzene)).

Synthesis of 1,4-Bis-bromomethyl-2,5-dimethylbenzene (4)

A solution of *p*-xylene (1.84 g, 17.4 mmol), paraformaldehyde (1.02 g), hydrogen bromide (5.1 M of acetic acid solution, 10 mL, 51.0 mmol), and acetic acid (8 mL) was stirred for 24 h at 60 °C. The reaction was monitored by TLC. The solution was neutralized with NaOH aqueous solution and washed with water several times, extracted by dichloromethane, and dried over MgSO_4 . Then, the solvent was removed *in vacuo*, and the desired material was purified by recrystallization from *n*-hexane to afford a white solid (0.907 g, 3.11 mmol, 18% yield).

^1H NMR (400 MHz, δ from TMS (ppm), CDCl_3): δ 2.36 (s, 6H, Ar-CH_3), 4.46 (s, 4H, $-\text{CH}_2\text{Br}$), 7.12 (s, 2H, 3,6H).

Synthesis of 1,4-Bis-(diethylphosphinoylmethyl)-2,5-dimethylbenzene (5)

A solution of 1,4-bis-bromomethyl-2,5-dimethylbenzene (0.805 g, 2.76 mmol), triethyl phosphite (1.05 mL, 6.25 mmol) was refluxed for 24 h at 120 °C, then unreacted triethyl phosphite was removed under reduced pressure. The desired material was purified by recrystallization from ethyl acetate to afford a pale yellow solid (0.878 g, 2.16 mmol, 78% yield).

^1H NMR (400 MHz, δ from TMS (ppm), CDCl_3): δ 1.24 (t, 12H, $-\text{OCH}_2\text{CH}_3$, $J = 7.3$ Hz), 2.31 (s, 6H, Ar-CH_3), 3.10 (d, 4H, $\text{Ar-CH}_2-\text{P-}$, $J_{\text{P-H}} = 20.6$ Hz), 3.98 (sept, 8H, $-\text{O-CH}_2-\text{CH}_3$, $J = 7.4$ Hz), 7.06 (d, 2H, 3,6H, $J = 1.4$ Hz).

Synthesis of CSCM Derivative (6)

Sodium methoxide (0.400 g, 7.40 mmol) was added in a solution of 1,4-bis-(diethylphosphinoylmethyl)-2,5-dimethylbenzene (0.296 g, 0.73 mmol) in DMF (3.5 mL) under N_2 atmosphere at 0 °C and stirred for 30 min. After change in

color from red to green, 4-(3,7-dimethyloctyloxy)benzaldehyde (0.389 g, 1.48 mmol) was added dropwise to the mixture and stirred for 2 h at rt. The reaction was monitored by TLC. Then, the mixture was washed with water, extracted by dichloromethane, and dried over MgSO_4 . After filtration, the solvent was removed *in vacuo*, and the crude product was purified by column chromatography (silica gel, chloroform). The compound was dried *in vacuo* to afford a light yellow solid (0.355 g, 0.57 mmol, 78% yield).

^1H NMR (400 MHz, δ from TMS (ppm), CDCl_3): δ 0.87 (d, 12H, $-\text{CH}(\text{CH}_3)_2$, $J = 6.8$ Hz), 0.95 (d, 6H, $-\text{CH}(\text{CH}_3)-\text{CH}_2-$, $J = 6.8$ Hz), 1.15–1.89 (m, 20H, $\text{O-CH}_2-\text{CH}_2-\text{CH}(\text{CH}_3)-(\text{CH}_2)_3-\text{CH}(\text{CH}_3)_2$), 2.41 (s, 6H, Ar-CH_3), 4.01 (td, 4H, $-\text{O-CH}_2-\text{C}_9\text{H}_{19}$, $J = 6.8$ Hz), 6.88 (d, 4H, 3,5H (side chain benzene) $J = 6.9$ Hz), 6.92 (d, 2H, Ar-CH=CH-Ar-O- , $J = 16.0$ Hz), 7.15 (d, 2H, Ar-CH=CH-Ar-O- , $J = 16.0$ Hz), 7.39 (s, 2H, 3,6H), 7.44 (d, 4H, 2,6H (side chain benzene), $J = 8.7$ Hz). MALDI-TOF MASS: calcd. for $\text{C}_{44}\text{H}_{62}\text{O}_2$, 622.96; found, 622.46.

CONCLUSIONS

We prepared PPV bearing π -conjugated side chains by Migita-Kosugi-Stille type polycondensation. The polymer exhibited broad optical absorption bands. The ESR measurements of the polymer during vapor-phase iodine doping revealed three phases of doping process. Charge carriers (polarons in the main chain and polarons in the side chains) are considered to be delocalized over the conjugated side chains and the main chains. This result implies two dimensionally directed polarons for the π -conjugated polymers.

The authors thank Chemical Analysis Division, Research Facility Center for Science and Technology, University of Tsukuba, and Glass Work Shop of University of Tsukuba. PL quantum efficiency measurements were carried out in Jasco (Japan).

REFERENCES AND NOTES

- 1 Walczak, R. M.; Leonard, J. K.; Reynolds, J. R. *Macromolecules* **2008**, *41*, 691–700.
- 2 Kim, J.; Paerk, S. H.; Kim, J.; Cho, S.; Jin, Y.; Shim, J. Y.; Shin, H.; Kwon, S.; Kim, I.; Lee, K.; Heeger, A. J.; Suh, H. *J. Polym. Sci. Part A: Polym. Chem.* **2011**, *49*, 369–380.
- 3 Kim, Y.; Bouffard, J.; Kooi, S. E.; Swager, T. M. *J. Am. Chem. Soc.* **2005**, *127*, 13726–13731.
- 4 Kokado, K.; Tokoro, Y.; Chujo, Y. *Macromolecules* **2009**, *42*, 9238–9242.
- 5 Dai, X. M.; Goto, H.; Akagi, K.; Shirakawa, H. *Synth. Met.* **1999**, *102*, 1289–1290.
- 6 Hu, Z.; Reichmanis, E. *J. Polym. Sci. Part A: Polym. Chem.* **2011**, *49*, 1155–1162.
- 7 Hsu, S.; Chen, C.; Wei, K. *J. Polym. Sci. Part A: Polym. Chem.* **2010**, *48*, 5126–5134.
- 8 Gong, X.; Ostrowski, J. C.; Moses, D.; Bazan, G. C.; Heeger, A. J. *J. Polym. Sci. Part B: Polym. Phys.* **2003**, *41*, 2691–2705.
- 9 Pei, J.; Yu, W.; Huang, W. *Macromolecules* **2000**, *33*, 2462–2471.
- 10 Letizia, J. A.; Salata, M. R.; Tribout, C. M.; Facchetti, A.; Ratner, M. A.; Marks, T. J. *J. Am. Chem. Soc.* **2008**, *130*, 9679–9694.

- 11** Babel, A.; Li, D.; Xia, Y.; Jenekhe, S. A. *Macromolecules* **2005**, *38*, 4705–4711.
- 12** Smilowitz, L.; Sariciftci, N. S.; Wu, R.; Gettinger, C.; Heeger, A. J.; Wudl, F. *Phys. Rev. B* **1993**, *47*, 13835–13842.
- 13** McGehee, M. D.; Miller, E. K.; Moses, D.; Heeger, A. J. In *Advances in Synthetic Metals: Twenty Years of Progress in Science and Technology*; Bernier, P.; Lefrant, S.; Bidan, G., Eds.; Elsevier Science: Switzerland, **1999**; pp 98–205.
- 14** Kawabata, K.; Goto, H. *Materials* **2009**, *2*, 22–37.
- 15** Ohkawa, S.; Ohta, R.; Kawabata, K.; Goto, H. *Polymer* **2010**, *2*, 393–406.
- 16** Li, Y.; Zou, Y. *Adv. Mater.* **2008**, *20*, 2952–2958.
- 17** Li, H.; Valiyaveetil, S. *Macromolecules* **2007**, *40*, 6057–6066.
- 18** Peeters, H.; Verbiest, T.; Koeckelberghs, G. *J. Polym. Sci. Part A: Polym. Chem.* **2009**, *47*, 1891–1900.
- 19** Hou, J.; Tan, Z.; He, Y.; Yang, C.; Li, Y. *Macromolecules* **2006**, *39*, 4657–4662.
- 20** Yu, C.; Ko, B.; Ting, C.; Chen, C. *Sol. Energy Mater. Sol. Cells* **2009**, *93*, 613–620.
- 21** Huang, F.; Tian, Y.; Chen, C.; Cheng, Y.; Young, A. C.; Jen, A. K.-Y. *J. Phys. Chem. C* **2007**, *111*, 10673–10681.
- 22** Huang, Y.; Wang, Y.; Sang, G.; Zhou, E.; Huo, L.; Liu, Y.; Li, Y. *J. Phys. Chem. B* **2008**, *112*, 13476–13482.
- 23** Brunner, K.; Tortschanoff, A.; Warmuth, C.; Bässler, H.; Kauffmann, H. F. *J. Phys. Chem. B* **2000**, *104*, 3781–3790.
- 24** Li, H.; Parameswaran, M.; Nurmawati, M. H.; Xu, Q.; Valiyaveetil, S. *Macromolecules* **2008**, *41*, 8473–8482.
- 25** Zou, Y.; Sang, G.; Wu, W.; Liu, Y.; Li, Y. *Synth. Met.* **2009**, *159*, 182–187.
- 26** Chiral polymers possess good film forming property in general.
- 27** Meyers, F.; Heeger, A. J.; Brédas, J. L. *J. Chem. Phys.* **1992**, *97*, 2750–2758.
- 28** Egbe, D. A. M.; Nguyen, L. H.; Hoppe, H.; Mühlbacher, D.; Sariciftci, N. S. *Macromol. Rapid Commun.* **2005**, *26*, 1389–1394.
- 29** Li, X.; Zhang, Y.; Yang, R.; Huang, J.; Yang, W.; Cao, Y. *J. Polym. Sci. Part A: Polym. Chem.* **2005**, *43*, 2325–2336.
- 30** Goto, H.; Iino, K.; Akagi, K.; Shirakawa, H. *Synth. Met.* **1997**, *85*, 1683–1684.
- 31** Zenin, A. A.; Feldman, V. I.; Warman, J. M.; Wildeman, J.; Hadziioannou, G. *Chem. Phys. Lett.* **2004**, *389*, 108–112.
- 32** Fernandes, M. R.; Garcia, J. R.; Schultz, M. S.; Nart, F. C. *Thin Solid Films* **2005**, *474*, 279–284.
- 33** Köse, M. E. *Theor. Chem. Acc.* **2011**, *128*, 157–164.